Array-Based GPR for Shallow Subsurface Imaging

A.G. Yarovoy, T.G. Savelyev, P.J. Aubry, L.P. Ligthart
International Research Centre for Telecommunications
and Radar, Delft University of Technology
Mekelweg 4, 2628 CD, Delft, the Netherlands
a.yarovoy@irctr.tudelft.nl

***Abstract*—Recently we have reported development of an UWB array-based time-domain Ground Penetrating Radar for landmine detection. The radar is designed to be used within a vehicle-mounted multi-sensor system for humanitarian demining and produces 3D images of subsurface by 1D mechanical scanning. In this paper, we demonstrate imaging capabilities of the developed system. The imaging capability of the radar is realized via electronic steering of the receive antenna footprint in cross-scan direction and synthetic aperture processing in along-scan direction. Imaging via footprint steering allows for drastic increase of the scanning speed.**

***Index Terms*—Video impulse radar, ultra-wideband antenna array, electronic footprint steering, subsurface imaging.**

I. Introduction

It has been demonstrated that ground penetrating radar (GPR) is a useful sensor for shallow subsurface investigation [1, 2]. Most complete information about subsurface can be extracted from GPR data if a GPR will perform a 2D scan over an area of interest. Migration of the acquired data allows not only to position properly all scatterers (including ones above the surface) but also create images of buried objects. Even for investigation of plane-layered structures (like roads or runways) 2D scan and data migration at a later stage gives more information than a single B-scan.

Surface survey by means of 2D mechanical scanning is a time-consuming process. Furthermore, positioning errors during mechanical movements of GPR (especially severe in cross-line direction) decrease considerably quality of reconstructed images. Thus a numerous attempts have been made to replace mechanical scanning in surface surveys by electronic scanning. In a traditional approach, 1D mechanical scan can be replaced by a linear array of transmit and receive antennas equally spaced along the array. In a traditional approach the number of transmit antennas equals to the number of receive antennas. Keeping in mind that for high resolution imaging of subsurface (e.g., for road or runway inspection or humanitarian demining) the scattered by subsurface field should be measured every 5-7cm in both horizontal directions, the antenna array requires a large number of transmit-receive antenna pairs. This results in a bulky antenna system and complicated hardware (see, e.g. [2, 3, 4]).

To avoid these problems, we suggest a novel approach to a system design [5, 6]. Firstly, the antenna array consists of a single transmit antenna and an array of receive antennas. The swath of such an array is limited by the footprint of the transmit antenna and the antenna array configuration. The scanning along the array is then done not by sequential measurements via different Tx/Rx antenna pairs but via focusing of the receive array footprint in the near-field and scanning with this footprint along the array. Such approach drastically reduces the data acquisition time, reduces the number of transmit antennas, simplifies the antenna system and considerably simplifies the electronics. Secondly, in order to improve the power budget of the radar at low frequencies (which are important for sufficiently deep penetration into the ground) we select a special waveform of the pulse fired by a generator. This waveform has a large spectral content at low frequencies to compensate for the decrease of the transmit antenna gain.

The paper is organized in the following way. System design and hardware are presented in Chapter 2. Results of the imaging of subsurface are presented in Chapter 3. Main outputs of the work are summarized in Chapter 4.

II. System Design

Developed by us array-based GPR comprises a pulse generator, an antenna array (with a single transmit antenna and 13 receive antennas), a seven-channel signal conditioner and an eight-channel sampling converter. The generator has also the second (calibration) output, which is used as a reference for compensation of time jitter and time drift. A block scheme of the array radar is shown in Fig. 1.

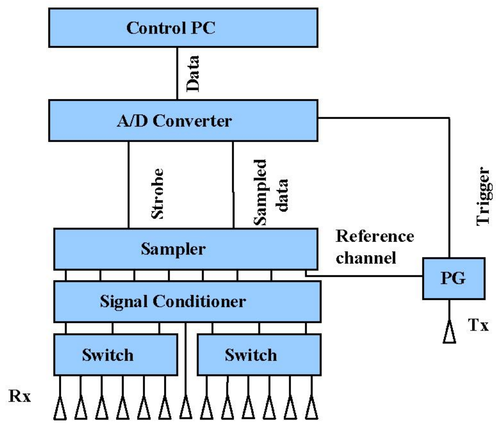

Fig. 1. Block scheme of the array radar.

1-4244-0887-3/07/$20.00 © 2007 IEEE

The generator fires a step pulse with a rise time of about 90ps. Such a waveform improves the radar power budget at low frequencies, which are not efficiently radiated by the transmit antenna due to the relatively small size of its physical aperture. Furthermore, the pulse repetition rate is of about 254 kHz, which allows for very fast data acquisition.

Within the antenna system we separated the transmit antenna and the receive array in the same way as we have done this in our previously designed radars [7, 8] in order to remove influence of the transmit antenna on the performance of the receive array and to decrease direct coupling between the transmit and receive antennas (which due to the finite dynamic range of a receiver limits the receiver sensitivity). As a result, the receive array is placed in H-plane of the transmit antenna with 27 cm separation between the transmit antenna aperture and the receive loops (Fig. 2).

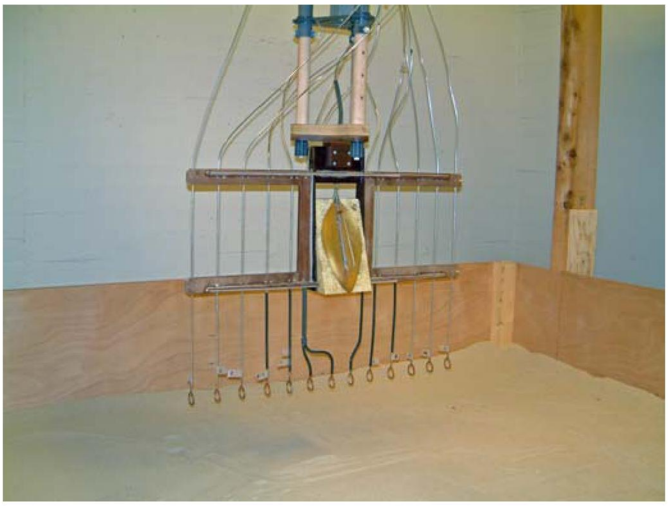

Fig. 2. Photo of the developed antenna array. The total aperture of the array is 84cm

The receiver chain consists of a seven-channel signal conditioner and an eight-channel sampling converter (built by GeoZondas Ltd., Lithuania). Ideally we would prefer to have the total number of receive channels in the sampling converter equal to the number of the receive antennas plus one (for the calibration purposes). However due to limited budget only 8-channel receiver has been built. The receiver chain has an analog bandwidth from 300MHz up to 6GHz and a linear dynamic range of 69dB (with averaging over 128 samples). The sampling converter operates with the sampling rate of 254kHz per channel, so all channels acquire signals due to each transmitted pulse simultaneously. The observation time window can be varied from 32ps till 20ns with a number of acquisition points available from 16 till 4096. The large flexibility in the duration of the observation time window and the sampling time allows us to adjust the system to different ground types and data acquisition scenarios. A very important feature of the sampling converter is its high measurement accuracy. The maximal error in the amplitude scale and the time scale linearity of the sampling converter is of about 1%.

An important part of the receiver chain is the signal conditioner. The signal conditioner improves the signal to noise ratio and allows to use the whole dynamic range of the ADC. The equivalent noise floor (which includes the discretization noise of ADC) of the receiver is less than 1.5mV RMS without averaging. The spectrum of the noise almost corresponds to white noise, so it can be efficiently suppressed by averaging. The signal conditioner decreases the noise floor and improves the signal-to-noise ratio by almost 30dB.

The long-term stability of the radar is characterized by the time-delay drift of about 12ps/hour. To improve the long term stability of the system the eighth channel of the sampling scope is used. This channel acquires one of two signals. For the time axis calibration a 4GHz harmonic signal from the internal generator of the sampling scope is acquired. For the delay drift compensation the reference signals from the generator is acquired. The data post-processing is used for compensation of the time drift based on the reference signals acquired in the eighth channel. As a result of this compensation, a time drift less than 1ps/hour has been achieved.

The noise floor of the system allows for a relatively low number of averages [5] to achieve a desirable value of the signal-to-noise ratio and thus very high data acquisition speed can be achieved.

The imaging procedure combines a synthetic aperture radar (SAR) algorithm with the digital steering of the receive array footprint. The synthetic aperture is being constructed in the direction of mechanical scanning for each array channel separately with a so-called diffraction stacking algorithm [9]:

$$s(t_k, x_l, y_m, z_n) = \sum_{channel=1}^{13} \sum_{j=1}^{N} s_{channel}(t_i, x_j, y_m, z_n) \quad (1)$$

where t_k is a travel time for the grid-point (x_l, y_m, z_n), t_i expresses travel time for the same depth grid-points (x_j, y_m, z_n). In this processing the coordinate system starts in the transmit antenna's phase centre: z-axis expresses depth, x-axis corresponds to the mechanical scan direction, y-axis represents the cross-scan direction. The travel times are computed as a two-way time delay between the transmit antenna, a grid-point and every receive antenna (Fig. 3). Every array channel is being focused onto line y_m after which we perform summation of the focused signals of all channels for this line.

In terms of phased antenna arrays summation of the channels represents digital synthesis of the array pattern with its maximum directed at (x_l, y_m, z_n). For the near-field case, it is equivalent to the digital steering of the array footprint. Instead of linearly progressive phase shift our footprint steering is based on the travel times which do not have a linear relationship between the array channels. Combination of SAR in the scan direction and footprint steering in the array's plane delivers a 3D image of a target.

Prior to imaging, we perform data pre-processing that includes low-pass filtering of the raw data to suppress

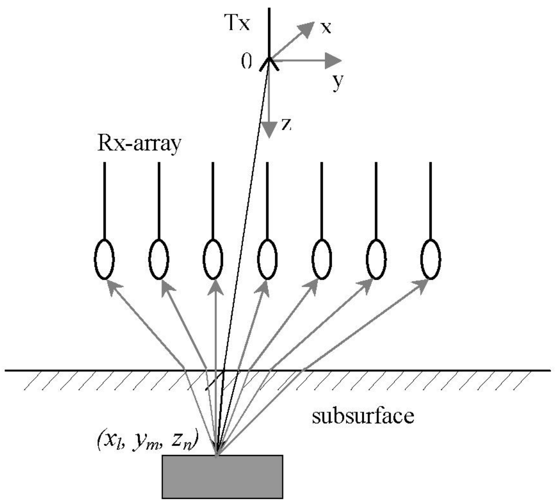

Fig. 3. Imaging geometry for the array GPR.

uncorrelated noise, alignment of the direct coupling in every B-scan to compensate for time drift, and background subtraction to remove direct coupling and ground surface reflection.

III. System Performance

Initial performance of the system has been tested in IRCTR test site for GPR antennas [10]. Typical target response is shown in Figure 4.

Different curves correspond to responses of different receive antennas within the array. The short duration of the transmitted signal results in high down-range resolution of the radar. The waveform of the target response keeps its shape while measured by different loops in the array. This feature is very important for application of the focusing algorithms to the measured data.

The spectrum of the target response keeps its shape while measured by different loops in the array (Figure 5). This feature is very important for the application of the focusing algorithms to the measured data.

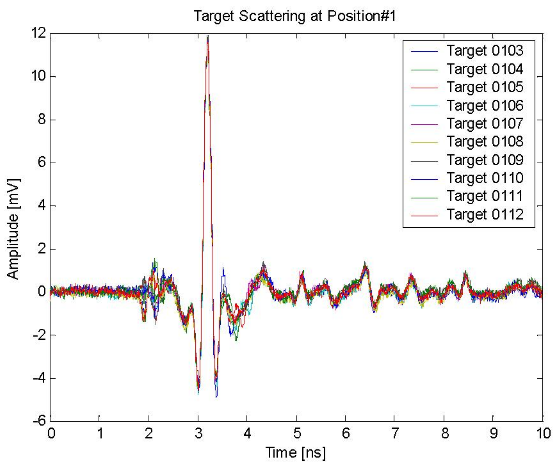

Fig. 4. Measured target response.

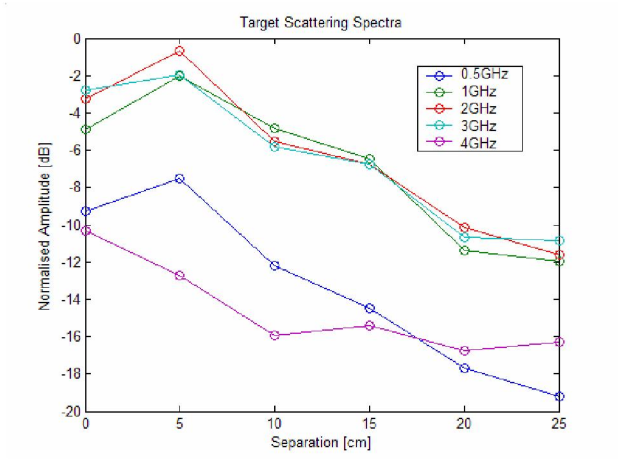

Fig. 5. Spectra of the target response.

Imaging capabilities of the developed system has been tested at TNO DS-S premises in The Hague [11]. The receive array has been elevated of about 20cm above the ground, which is a dry sand. The measured dielectric permittivity of the sand is 3.03.

Figure 6 illustrates a resolution capability of the array. Two metal discs of 5 cm diameter placed on the ground surface and separated by 7 cm between the edges are completely resolved. The minimum intensity between two images is more than 20dB below the intensity in the centers of the disks. Furthermore, it is still possible to resolve the discs for 5 cm separation at -6dB level.

Figure 7 demonstrates a capability of the array to image buried landmines. Two PMN-2 landmines were buried in dry sand at a depth of 5 cm. One mine is in the middle of the imaging strip, the other is at the rightmost position. The both targets can be clearly seen.

Despite the landmines are identical their images look different due to difference in energy received from a target under the transmit antenna and from a target which is close to the array's edge.

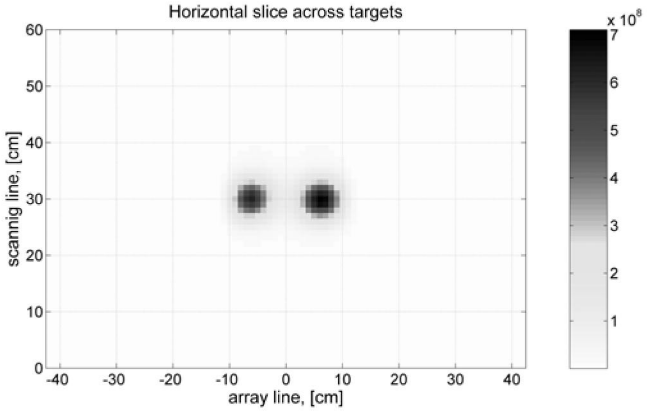

Fig. 6. Image of 2 metal discs with 5cm diameter separated by 7 cm. Image intensity is in a linear scale.

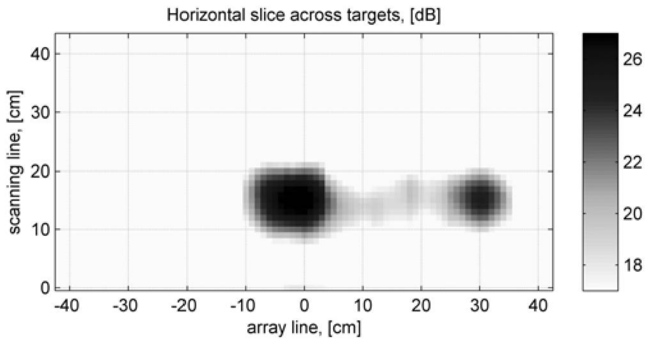

Fig. 7. Image of 2 PMN2 antipersonnel landmines buried at a depth of 5cm in sand. Image intensity is given in dBs.

IV. Conclusion

A novel approach for an array-based imaging radar has been proposed. The approach comprises the system design with a single transmitter and multi-channel receiver, design of a receive antenna array, and selection of a special waveform fired by the pulse generator. The proposed approach aims at realization of fast 3D imaging of subsurface by one-dimensional mechanical scanning over it. Drastic improvement in the scanning speed over the existing systems should be gained by electronic steering of the receive antenna footprint in cross-scan direction. At the same time the suggested approach considerably simplifies the radar sensor in general and its antenna system compared to the known array GPR.

The approach has been verified experimentally by manufacturing a "proof-of-principle" demonstrator based on the time-domain technology. The application in mind is humanitarian demining. The radar possesses a bandwidth of about 3.56GHz and the operational band starts at 240MHz. This results in combination of fine down-range resolution with sufficient penetration into the ground for detection of buried targets. Using the near-field footprint formation in the cross-scan direction and synthetic aperture focusing in the scan direction, the radar provides 3D focused images of the near-field area. First experimental results show that the system successfully images different metal and dielectric objects within the aperture of the antenna array.

The maximal scanning speed of the system is 148km/h, which is almost two orders of magnitude higher than by existing systems. The cross-range resolution of the images is of about 5cm, which is sufficient for such an application as humanitarian demining. The swath of these images is of about 84cm. Combination of the above mentioned figures of merits allows to say about a technological breakthrough in the field.

Acknowledgment

The authors would like to thank Dr. B. Levitas from Geo-Zondas Ltd., Vilnius, Lithuania, for fruitful cooperation and help during the development of the radar electronics and J.H. Zijderveld, P. Hakkaart and M. v.d. Wel from Delft University of Technology for their technical assistance during antenna measurements, system assembling and testing.

References

[1] E. Eide, P.-A. Sandnes, B. Nilssen, S. Tjora, "Airfield runway inspection using 3 dimensional GPR," *Proc. the 3rd International Workshop on Advanced Ground Penetrating Radar (IWAGPR)*, May, 2005, Delft, The Netherlands, pp. 87-91.

[2] R.J. Chignell, and M. Hatef, "LOTUS – a Real Time Integrated Sensor Suite for Anti-Personnel Mine Detection, Incorporating the MINEREC GPR," *Proc. Xth Int. Conf Ground Penetrating Radar*, 21-24 June 2004, Delft, the Netherlands, pp. 665-668.

[3] E.S. Eide, J.F Hjelmstad, "A multi antenna ultra wideband ground penetrating radar system using arbitrary waveforms," *IGARSS'99 Proceedings*, Hamburg, Germany, vol.3, pp. 1746-1748, 1999.

[4] T. Hansen et al., "Efficient large-scale underground utility mapping with a multi-channel ground-penetrating imaging radar system," *General Assembly URSI, Proceedings*, Maastricht Exhibition and Congress Centre (MECC), Maastricht, The Netherlands, 17-24 August 2002, 4p., 2002.

[5] A. Yarovoy, T. Savelyev, P. Aubry, P. Lys and L. Ligthart, "UWB Array-Based Sensor for Near-Field Imaging," to be published in *IEEE Trans. MTT*, vol. 55, no. 6, 2007.

[6] A. Yarovoy, P. Aubry, P. Lys and L. Ligthart, "Array-Based GPR for Landmine Detection," *Proc. XIth Int. Conf. Ground Penetrating Radar*, Columbus Ohio, 19-22 June 2006, pp. 1-6.

[7] A.G. Yarovoy et al., "Ground penetrating impulse radar for detection of small and shallow-buried objects," *IGARSS'99 Proceedings*, Hamburg, Germany, vol.5, pp.2468-2470, June 1999.

[8] A.G. Yarovoy, L.P. Ligthart, A. Schukin, and I. Kaploun, "Polarimetric Video Impulse Radar for Landmine Detection," *Subsurface Sensing Technologies and Applications*, vol.3, no.4, pp.271-293, Oct. 2002.

[9] J. Groenenboom, and A.G.Yarovoy," Data processing and imaging in GPR system dedicated for landmine detection," *Subsurface Sensing Technologies and Applications*, vol.3, no.4, pp.387-402, Oct. 2002.

[10] Yarovoy, A.G., "Comprehensive Experimental Analysis of GPR Antennas," *Proc. the Tenth International Conference on Ground Penetrating Radar*, Delft, The Netherlands, vol. 1, pp.153-156 (2004).

[11] V. Kovalenko, A. Yarovoy, L.P. Ligthart, P. Hakkaart, and J. Rhebergen, "Joint IRCTR / TNO-DS&S measurement campaign for AP-mine detection with VIR GPR", *Proc. the 3rd International Workshop on Advanced Ground Penetrating Radar (IWAGPR)*, May, 2005, Delft, The Netherlands, pp. 31 – 36.